INSTITUTE OF PHYSICS PUBLISHING INVERSE PROBLEMS

Inverse Problems 22 (2006) 43–53 doi:10.1088/0266-5611/22/1/003

Electromagnetic source localization in shallow waters using Bayesian matched-field inversion

Marius Birsan

Defence Research & Development Canada Atlantic, 9 Grove Street, PO Box 1012, Dartmouth, Nova Scotia, B2Y 3Z7 Canada

E-mail: Marius.Birsan@drdc-rddc.gc.ca

Received 14 March 2005, in final form 17 November 2005
Published 22 December 2005
Online at stacks.iop.org/IP/22/43

Abstract

The propagation of an electromagnetic signal in a marine environment cannot be modelled as a plane wave due to the high attenuation in seawater and the interactions with the ocean boundaries. Consequently, conventional beamforming techniques are not applicable for electromagnetic source localization. In this work, the Bayesian approach to matched-field processing is used to localize an electromagnetic source and estimate the environmental parameters. In this formulation, the solution to the inverse problem is given by the *a posteriori* probability distribution calculated here using the Gibbs sampling method. Bayesian inversion theory provides the formalism for estimating parameters, their uncertainties and verification of the estimates convergence. Two situations were investigated for the case where the single frequency measurements represent the magnitudes of two orthogonal horizontal electric field components: (1) all environmental parameters known and (2) unknown seabed conductivity. The objective function that relates the array data to the propagation model and environment parameters was chosen for the practical situation considered.

Introduction

A vessel will generate time-varying electromagnetic (EM) fields because of the various propulsion and power systems onboard. The resulting EM fields from a vessel represent its extremely low frequency (ELF) signature. Understanding the ELF electromagnetic signature is important since it can be used as a method of detecting and localizing a vessel. The attenuation of the electromagnetic field in seawater is large, and the range of detection/localization methods that exploit the ELF signature is therefore limited. These methods, however, may be useful in shallow seawater environments (10–30 m) where the acoustic methods are often inadequate due to reverberation and environmental noise.

0266-5611/06/010043+11$30.00

The localization of a low-frequency narrow-band EM source in the wave-guide represented by shallow water should involve an array processing method that incorporates the physics of wave propagation as an integral part of the solution. The use of the precise full wave propagation model is motivated by the air–seawater and seawater–seabed interfaces whose presence cannot be neglected. The shallow water environment is modelled as a layered structure with parameters that change in the vertical direction. EM source localization in a layered structure represents a strongly nonlinear inverse problem with no direct solution. A matched-field processing (MFP) approach to this problem is formulated by minimizing an error function that quantifies the mismatch between the measurement vector and the steering or replica vector derived from a solution of the wave equation. Historically, the MFP method has been extensively applied in acoustics to the problem of underwater passive source localization [1]. Beyond acoustic applications, MFP techniques are currently being explored for problems involving multi-path electromagnetic propagation. Although this work is still in its early stages, electromagnetic MFP has already been proposed in several applications, such as aircraft height determination using low-angle radar [2], source localization and inversion of tropospheric refractivity [3] and target localization in over-the-horizon radar [4].

Electromagnetic field propagation in a marine environment is a topic extensively studied in our laboratory. To a large extent, the interpretation of the experimental data in this area makes use of the propagation model developed by Weaver [5], where it is assumed that, at least within a limited range, the marine environment can be modelled by a set of horizontal layers. The Weaver model has been validated by many experiments. An example of such an experiment is presented in [6]. One of the electromagnetic sources used in this experiment was a horizontal electric dipole (HED), 25 m long placed on the sea bottom 260 m away from an array of five vector sensors for voltage detection. All the parameters, geometric and environmental, of the experiment were known and presented in [6]. The magnitudes of the electric field components measured in the longitudinal and transverse directions (relative to the direction of the sensor array) were in good agreement with the predicted values. An attempt to invert the problem and infer the geometrical and/or environmental parameters from the measurements using conventional matched-field processing raised interesting questions related to the uncertainties in the parameter estimation, which make the subject of this paper.

An important practical problem in matched-field inversion is to quantify the information content of the unknown model parameters. A solution to this problem, first applied by Gerstoft [7] and Gerstoft and Mecklenbrauker [8] to geoacoustic inversion, makes use of the Bayesian formalism. In this formulation, the information content of each parameter can be quantified in terms of its marginal posterior probability distribution (PPD), which defines the accuracy expected in inversion.

The objective of this work is to investigate to what extent the MFP technique can be used for determining environmental and geometrical parameters of the low-frequency EM source localization problem in shallow seawater. To address this problem, an existing inversion methodology (the Gibbs sampling method) developed in ocean acoustic by Dosso [9–11] is applied to estimate the model parameters and their uncertainties. The approach is exercised on real data obtained during an experiment where we have some *a priori* knowledge about the geometry and environmental settings.

Basic concepts of Bayesian MFP

Matched-field processing is a generalized beamforming technique where the field predictions for propagating signals are obtained as the full field solution of the wave equation in a ducted channel. The difference between this technique and the conventional narrow-band plane-wave

beamforming is that the 'replica vectors' derived from the spatial point source response of the medium replace the array weights based on plane wave 'steering vectors'. In the simplest terms, MFP searches a multi-dimensional model parameter space to obtain the best fit between the measured and the modelled (replica) data obtained from the wave equation. The correlation between the predicted field values, $\mathbf{w}(\mathbf{m})$, obtained from the forward propagation model, and the measured data, $\mathbf{d}$, is realized by the objective function.

Being a beamforming technique, MFP requires a set of spatial samples of the signal field from an array of sensors. In this study, the data represent the measured amplitudes of the EM field at an array of N vector sensors due to a horizontal electric dipole (HED) located in a layered structure. A low-frequency (quasi-static) propagation model [5] is used to calculate the complex EM field at the sensors for many sets of trial environmental/geometric model parameters. The errors between the EM field at the receiving array and the predicted values are assumed complex Gaussian distributed with zero mean and diagonal covariance matrix $\upsilon\,\mathbf{I}$.

A brief description of the Bayesian theory applied to MFP is presented here that follows the rigorous likelihood-based approach developed in [8–12]. In the Bayesian formulation, the result of inversion is the *a posteriori* probability density, $P(\mathbf{m}|\mathbf{d})$, of the model parameter vector, $\mathbf{m} = \{m_1, m_2, \ldots, m_M\}$, given the observed data vector, $\mathbf{d}$. The vector $\mathbf{d} = \{d_1, d_2, \ldots, d_n, \ldots, d_N\}$ has elements consisting of the amplitude of the electric field measurements, and $|\mathbf{d}|$ is the magnitude of vector $\mathbf{d}$. The *a posteriori* probability distribution function (PDF) represents the state of information of $\mathbf{m}$ given the *a priori* information of the model independent of the data, $P(\mathbf{m})$, and the information provided by the data (Bayes theorem):

$$P(\mathbf{m}|\mathbf{d}) \propto L(\mathbf{d}|\mathbf{m})P(\mathbf{m}), \tag{1}$$

where $L(\mathbf{d}|\mathbf{m})$ is the likelihood function. The form of the data and the statistical distribution of the data errors determine this function. Let us assume complex additive Gaussian distributed errors on the electric field at N sensors and unknown source magnitude. Under these assumptions, the electric field amplitude at each sensor has a Riccian probability density [12] giving the log-likelihood function for an N-element array at a single frequency:

$$\Lambda(\mathbf{m}) = -N\log\upsilon - \frac{|\mathbf{d}|^2 + S^2|\mathbf{w}(\mathbf{m})|^2}{\upsilon} + \sum_{n=1}^{N} \log I_0\left(\frac{2|w_n(\mathbf{m})Sd_n|}{\upsilon}\right), \tag{2}$$

where S represents the unknown source strength, and $I_0(x)$ is the modified Bessel function of first kind and zero order. Equation (2) is simplified in the case of high SNR when the approximation of the Bessel function $I_0(x) \approx \exp(x)$ can be used:

$$\Lambda(\mathbf{m}) \cong -N\log\upsilon - \frac{|\mathbf{d}|^2 + S^2|\mathbf{w}(\mathbf{m})|^2}{\upsilon} + \frac{2S}{\upsilon}\sum_{n=1}^{N} d_n w_n(\mathbf{m}). \tag{3}$$

Writing the likelihood function as

$$L(\mathbf{d}|\mathbf{m}) \propto \exp(-E(\mathbf{m})), \tag{4}$$

where $E(\mathbf{m})$ represents the error function, and maximizing the log-likelihood function (3) relative to S, one obtains

$$S = \frac{\mathbf{d}^{\mathrm{T}}\mathbf{w}(\mathbf{m})}{|\mathbf{w}(\mathbf{m})|^2}, \tag{5}$$

$$E(\mathbf{m}) = \left[|\mathbf{d}|^2 - \left(\frac{|\mathbf{d}^{\mathrm{T}}\mathbf{w}(\mathbf{m})|}{|\mathbf{w}(\mathbf{m})|}\right)^2\right] \Big/ \upsilon = B(\mathbf{m})/\upsilon, \tag{6}$$

where $B(\mathbf{m})$ is the Bartlett power mismatch function, and T indicates the transpose.

One advantage of applying the Bayesian formalism to inverse problems is that it includes the data uncertainties, both measurement and theoretical errors, into the solution. In general, information about the statistical distribution of the measured EM field is not available *a priori*. However, the data variance can be estimated [8] by substituting equation (5) in (3) and then optimizing with respect to υ. The solution is

$$\hat{\upsilon} = B(\mathbf{m}^{\mathrm{ML}})/N, \tag{7}$$

where the maximum likelihood (ML) model, $\mathbf{m}^{\mathrm{ML}}$, is found by minimizing the mismatch function using a global optimization procedure.

An effective method to calculate the marginal probability distribution of the parameters in the Bayesian inversion is based on the simulated annealing (Metropolis) algorithm at constant temperature, $T = 1$. The algorithm implements the (importance) Gibbs sampling method and provides an estimate of the posterior distributions in an efficient manner. It was shown [9] that after a suitable large number of accepted perturbations in the simulated annealing algorithm, the sampling distribution of the unknown parameters, $G(\mathbf{m})$, is given by the Gibbs PDF. Moreover, the two functions, the Gibbs PDF at constant temperature, $T = 1$, and the PPD characterizing the solution of an inverse problem are identical in the case of uniform prior distribution, which is the standard case in MFP.

When the Gibbs sampler provides a probability distribution function, $G(\mathbf{m})$, representing an unbiased sampling of the PPD

$$P(\mathbf{m}|\mathbf{d}) = G(\mathbf{m}) \tag{8}$$

the moments such as the mean, covariance and marginal distributions, which provide parameter estimates and uncertainties, can be estimated as

$$\begin{aligned} \langle \mathbf{m} \rangle &= \int G(\mathbf{m})\mathbf{m}\,\mathrm{d}\mathbf{m} \qquad \mathrm{cov}(\mathbf{m}) = \int G(\mathbf{m})(\mathbf{m} - \langle \mathbf{m} \rangle)(\mathbf{m} - \langle \mathbf{m} \rangle)^{\mathrm{T}}\,\mathrm{d}\mathbf{m} \\ P(m_j|\mathbf{d}) &= \int G(\mathbf{m})\,\mathrm{d}m_1, \ldots, \mathrm{d}m_{j-1}\,\mathrm{d}m_{j+1}, \ldots, \mathrm{d}m_M. \end{aligned} \tag{9}$$

Electromagnetic propagation model

In the following, the EM source is a horizontal electric dipole (HED) located in the seawater that radiates a narrow band, continuous sine wave. Since MFP exploits the environment, the forward propagation model must be accurate, especially when one seeks high performance. To obtain the time-varying EM field at the sensors located in the shallow seawater, one must solve Maxwell's equations for a dipole in a stratified media where there are two lateral wave modes of propagation—lateral waves that propagate on the sea surface and along the seabed. The EM propagation modelling [5] is done in the frequency domain for very low frequencies where the quasi-static approximation (displacement current neglected) is valid.

The ocean environment for the forward model consists of three horizontal layers: air, seawater and seabed. The electromagnetic properties of each layer are considered to be homogeneous, linear and isotropic. It is understood that the magnetic permeability μ_i for each layer can be replaced by the constant $\mu = \mu_0$, the permeability of the free space. Since we are considering time-harmonic cases, it is noted that the time factor $\exp(\mathrm{j}\omega t)$ is used for the field quantities in the frequency domain and is omitted throughout.

The x and y directions denote the horizontal plane. This is the plane in which the structure is uniform in its electromagnetic parameters. The z direction is the vertical direction pointing downwards in which the structure varies in its properties. The origin of this Cartesian

reference frame is located on the interface of air and seawater. A semi-infinite conducting medium occupies the half-space $z > 0$ of a rectangular coordinate system (x, y, z) and has the conductivity σ_1 for $0 < z < d$, and σ_2 for $z > d$, where d is the sea depth. The region $z < 0$ is taken to be free space. The position of the current dipole has the coordinates $x = y = 0$, $z = h$ $(0 < h < d)$. It is convenient to introduce cylindrical polar coordinates (ρ, θ, z) with $x = \rho\cos\theta$, $y = \rho\sin\theta$.

As shown by Weaver [5], this problem is solved by applying Maxwell's equations in each of the three regions, air–seawater–seabed. The magnetic $\mathbf{H}$ and electric $\mathbf{E}$ fields are written as functions of the vector potential $\mathbf{A}$:

$$\mathbf{H} = \nabla \times \mathbf{A} \qquad \mathbf{E} = -\mathrm{j}\omega\mu\,\mathbf{A} + \frac{1}{\sigma}\nabla\nabla\cdot\mathbf{A}, \tag{10}$$

where ω is the frequency and σ is the conductivity of the medium. The vector potential $\mathbf{A}_k$, in medium k $(k = 0, 1, 2)$, must satisfy the equation

$$\nabla^2\mathbf{A}_k - \mathrm{j}\omega\mu\sigma_k\mathbf{A}_k = -D_k\delta(r_0), \tag{11}$$

where D_k is the strength of the dipole, $D_0 = D_2 = 0$, $\sigma_0 = 0$ in air and $\mathbf{r}_0$ is the distance from the source to the field point. The boundary conditions require that the magnetic field and the tangential component of the electric field are continuous across the boundaries

$$\begin{aligned} &\mathbf{n}\cdot\nabla\times(\mathbf{A}_k - \mathbf{A}_{k+1}) = 0, \qquad \mathbf{n}\times\nabla\times(\mathbf{A}_k - \mathbf{A}_{k+1}) = 0 \\ &\mathbf{n}\times\nabla\nabla\cdot\left(\frac{\mathbf{A}_k}{\sigma_k} - \frac{\mathbf{A}_{k+1}}{\sigma_{k+1}}\right) = 0, \end{aligned} \tag{12}$$

where $\mathbf{n}$ is the unit vector of the exterior normal to the surface.

In the case of a horizontal electric dipole, the vector potential must have both x- and z-components, $\mathbf{A}_k = \mathbf{x}A_{k,x} + \mathbf{z}A_{k,z}$, to satisfy the above boundary conditions. Weaver derived the solution $\mathbf{A}_1$, in medium 1 (seawater). Explicit expressions can be found in [5]. For example, $A_{1,X}$ is written below using a slightly different notation from Weaver:

$$\begin{aligned} A_{1,X} = {} & \frac{D_1}{4\pi r_0}\exp(-\alpha_1 r_0\sqrt{\mathrm{j}}) + \frac{D_1}{4\pi}\int_0^\infty \mathrm{d}\lambda\,\frac{\lambda}{\sqrt{\lambda^2 + \mathrm{i}\alpha_1^2}}\,J_0(\rho\lambda) \\ & \times\left\{F\exp\left[-(z+h)\sqrt{\lambda^2 + \mathrm{j}\alpha_1^2}\right] + P\exp\left[-(2d - z - h)\sqrt{\lambda^2 + \mathrm{j}\alpha_1^2}\right]\right\}, \end{aligned} \tag{13}$$

where we have put $\alpha_1 = \sqrt{(\mu\omega\sigma_1)}$ and J_0 denotes the Bessel function of the first kind and zero order. The expression for P was determined from the boundary condition

$$P = \frac{G}{1 - FG\exp\left(-2d\sqrt{\lambda^2 + \mathrm{j}\alpha_1^2}\right)}\left[1 + F\exp\left(-z\sqrt{\lambda^2 + \mathrm{j}\alpha_1^2}\right)\right]\left[1 + F\left(-2h\sqrt{\lambda^2 + \mathrm{j}\alpha_1^2}\right)\right]. \tag{14}$$

Here, we have defined the reflection coefficients for the seawater–air and seawater–seabed interfaces, respectively:

$$F = \frac{\sqrt{\lambda^2 + \mathrm{j}\alpha_1^2} - \lambda}{\sqrt{\lambda^2 + \mathrm{j}\alpha_1^2} + \lambda}, \qquad G = \frac{\sqrt{\lambda^2 + \mathrm{j}\alpha_1^2} - \sqrt{\lambda^2 + \mathrm{j}\alpha_2^2}}{\sqrt{\lambda^2 + \mathrm{j}\alpha_1^2} + \sqrt{\lambda^2 + \mathrm{j}\alpha_2^2}}. \tag{15}$$

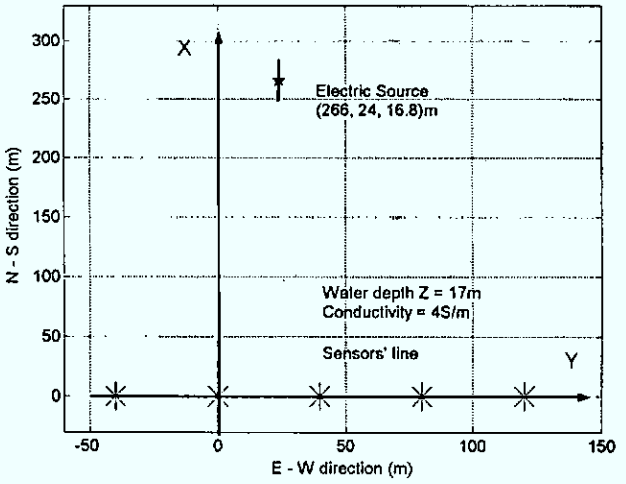

Figure 1. Setting of the EM propagation experiment.

Experiment and results

The EM propagation experiment was carried out in the Esquimalt harbour, British Columbia, and its geometry is shown in figure 1. The experiment consisted of recording electric field data at a horizontal line array of five vector sensors placed on the seabed due to a horizontal electric source also placed at the bottom of the sea, about 260 m away from the array. The array endpoints are on the Y-axis, the sensors are placed 40 m apart, and the origin of the middle sensor has the coordinate (0, 40, 16 m). All sensors are assumed to be identical. When real data are used, one must acknowledge the errors in the geometrical parameters due to the positioning inaccuracy, especially when all the equipment is placed underwater on an uneven seabed. The errors in the position of the sensors, their alignment and orientation, as well as the errors in the source position and orientation, imply that the 'true' values in this paper are only approximated.

The source (a 25 m long wire) emitted a continuous sine wave with frequencies between 1 and 256 Hz. The environmental parameters available from direct measurement were the seawater depth and conductivity. The value of the seabed conductivity was initially estimated from a trial and error procedure to obtain the best agreement between the measured magnitudes of the x and y electric field components and the predicted values for all the frequency range from 1 to 256 Hz. The parameters, geometric and environmental, of the experiment are estimated to be [6]

- source position: $x = 266$ m, $y = 24$ m, $z = 16.8$ m, orientation angle = 10°,
- dipole moment = 33.6 A m,
- water depth = 17 m, water conductivity = 4 S m^{-1}, bottom conductivity = 0.2 S m^{-1} and
- SNR of 30 dB.

To investigate the MFP performances for the EM source localization, only a single frequency inversion for the model described above is performed. Figure 2 presents the comparison between experimental and calculated values at 32 Hz. Using these data and the Bayesian approach to the MFP method, we attempted to determine four parameters that give the source position and orientation: x, y and z coordinates and the dipole orientation angle.

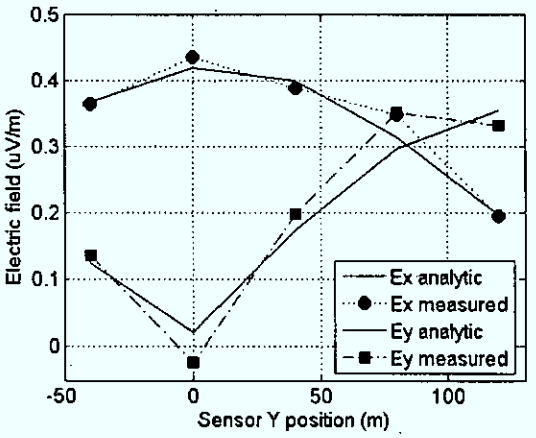

Figure 2. Measured and predicted x and y electric field components along the sensor array.

Reasonably wide parameter search bounds ($0 \leqslant x \leqslant 500$ m, $-200 \leqslant y \leqslant 200$ m, $1 \leqslant z \leqslant 16.8$ m and $-90° \leqslant$ orientation angle $\leqslant 90°$) were adopted to assess the resolving power of the EM data with limited prior information. For meaningful results it is necessary to verify that the estimates have converged. Convergence was established by collecting two independent samples in parallel and periodically comparing the PPD moments estimated from each sample [9]. The procedure is terminated when the difference between two cumulative marginal distributions for all parameters is less than 0.1.

In the first inversion performed, the seabed conductivity was assumed as known ($0.2\ \mathrm{S\ m^{-1}}$) and the case involved four unknown geometrical source parameters: x, y, z and orientation angle. To speed up the convergence, the sampling algorithm was initiated at high temperature and cooled rapidly to $T = 1$ to ensure that the sampling begins at models that are highly probable. The models selected during the cooling process were not retained in the sample. Then the Gibbs sampling algorithm evaluated approximately 5×10^4 models before the estimation of the marginal PPDs converged. The computation required about 2 h of CPU time on a single processor 850 MHz Pentium PC mainly because of the time necessary to compute the forward propagation model. Except for the initial cooling stage, no other method was used to increase the efficiency of the sampling algorithm. In a more computationally intensive inverse problems with many unknown parameters, such as the multi-frequency inversions in ocean acoustic, two additional methods were used to accelerate the convergence of the Gibbs sampler [9]: (a) the perturbations were applied in a rotated model space obtained by diagonalizing the parameter covariance matrix and (b) the maximum perturbation sizes were determined using a simple adaptive scheme.

The *a posteriori* distributions and the 'true' values (the true value for z is 16.8 m) for the four parameters are shown in figure 3. The marginal distributions throughout this paper are plotted as histograms of the sampled models discretized into 50 bins and scaled so that the total area is one when the search interval is scaled from 0 to 1. The parameter plot limits are reduced to better illustrate the structure of the distribution. It is worth mentioning that whatever normalization is applied, it does not preclude comparisons between parameters or figures since the interpretation of parameter uncertainties is based on the relative width rather than amplitude. The source locations have well-defined compact distributions with maxima very close to the true values, except for the z coordinate that practically cannot be determined.

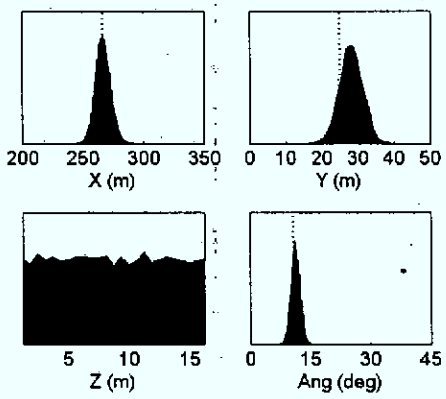

Figure 3. Estimated marginal PPDs to localize the EM source from experimental data.

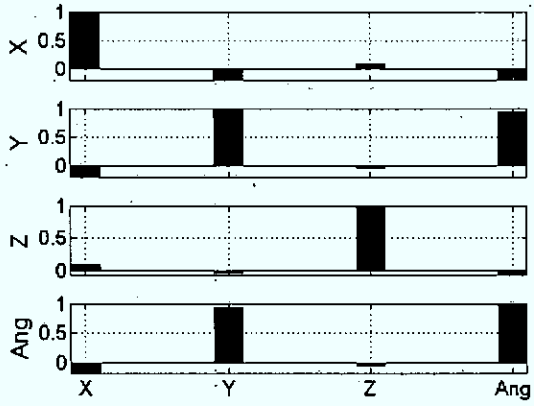

Figure 4. Correlation matrix for geometrical parameters.

The difference between the true value and the mean value of the estimated y position, which is 28.22 m, may be attributed to the inherent errors in the experimental setting.

Another possible cause for the inaccuracy of the estimates is the parameter coupling. To examine the parameter inter-dependences, it is advantageous to use the normalized elements of the covariance matrix because the parameter scales and units do not affect them (equation (30) in [9]). The correlation matrix estimated using the measured data is given in figure 4. This figure indicates that reasonably strong positive correlation exists between the y position and the source orientation angle, which is due to the geometry of the experiment. The x position of the source relative to the sensors is much higher than y (at least for a couple of sensors), so that small perturbations of the angle between the x-axis and the dipole heading will generate large fluctuations in the y-component of the field. The x and z coordinates of the source are practically independent.

This result prompted more investigation using synthetic data. Several sets of the magnitudes of all three electric field components, x, y and z, were generated using the forward model with the source placed at smaller distances relative to the sensors in the same

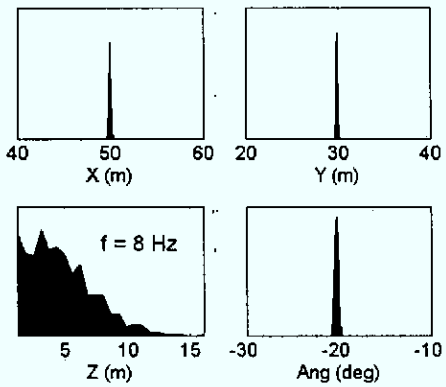

Figure 5. Marginal PPDs obtained from synthetic data.

environment as above. White Gaussian noise was added to the data vectors to obtain an SNR of 30 dB. For the geometry of the experiment, the magnitude of the z-component of the electric field is two orders of magnitude smaller than the magnitude of the horizontal components. Only when the source is brought close to the sensors so that the magnitudes of the three electric field components are of the same order of magnitude, the z-coordinate can be resolved. An example of inversion using the synthetic data with the source in an intermediate position is shown in figure 5. The source emitting an 8 Hz sine wave is placed at (50, 30, 5 m) with an azimuth angle of –20°. Being closer to the sensors and at lower elevation, the magnitude of the z-component of the field is increased relative to the horizontal components, and the estimate of the z-coordinate has a better resolution. The estimated x, y and orientation angle correspond to the true values and the convergence of inversion is much faster. By comparing these results, one can conclude that there are errors in the assessment of the experimental settings (sensors and source positions, orientations, alignment) due to an incomplete forward model (seabed irregularities).

If the environmental parameters are not known, it is in general not possible to estimate the source position. Using wrong values for seawater depth and conductivity and seabed conductivity can seriously degrade the performance and give a wrong estimate of the source localization. Fortunately, the conductivity and the thickness of the seawater layer are usually known with a high degree of accuracy. An environmental parameter difficult to evaluate is the seabed conductivity because it represents the average value over the region where the experiment takes place. Moreover, for the geometry used in this experiment with the source and the sensors placed close to sea floor, the field penetrates into the seabed to a certain depth making the conductivity measurements practically impossible. Instead of estimating its value from a trial and error procedure as before, it could be estimated from the field measurements using matched-field inversion.

Because the z-coordinate cannot be evaluated, the parameters used for inversion are the x and y coordinates, the source orientation angle and the seabed conductivity. The z coordinate was set to an arbitrary value of 8.5 m. Figure 6 illustrates the *a posteriori* distributions for the four parameters together with the initially estimated (true) values (dotted lines). The distributions were obtained using the Gibbs sampling method as before, which evaluated about 5×10^4 models until reaching convergence. The distributions are well defined and the mean values of the parameters are 255.56 m, 20.6 m, 6.99° and 0.37 S m^{-1}. In this

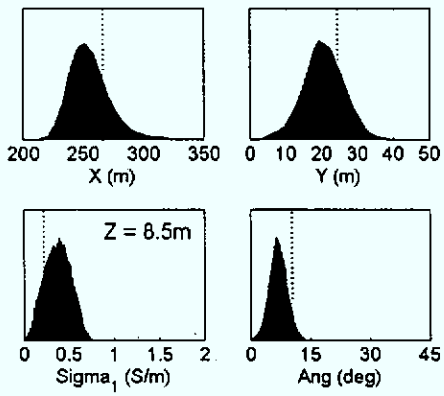

Figure 6. Estimated marginal PPDs for source x, y and orientation and seabed conductivity.

case, the estimated parameters are slightly different in comparison with the previous inversion parameters obtained with constant bottom conductivity (0.2 S m^{-1}).

Conclusions

The nonlinear electromagnetic inversion problem was solved to localize an electric source in a marine environment and to estimate the environmental parameters. The study focused on quantifying the information content of each unknown parameter in terms of its marginal *a posteriori* probability distribution using the Bayesian theory of inversion. At this moment, applying the Bayesian theory to the MFP method is not practical from the computational point of view, especially when a real-time inversion is desired. The reason is the calculation of the replica vector that requires most of the computation time. However, by using the Bayesian inference theory for estimating parameter uncertainties one can determine which parameters are well determined in an application.

Using the MFP and measured data, a horizontal electric source was localized with reasonable accuracy (given the experimental conditions) in the horizontal plane. The z coordinate cannot be resolved for the geometry considered in this experiment, because of the small value of the z field component that practically does not affect the inversion. Also, the seabed conductivity, a parameter difficult to evaluate from measurements, can be estimated by inversion. The results presented in this paper show that the EM matched-field processing methods can be used for source localization in a marine environment and reveal a promising method to localize a ship using its ELF signature.

References

[1] Baggeroer A B, Kuperman W A and Mikhalevsky P N 1993 An overview of matched field methods in ocean acoustic *IEEE J. Ocean. Eng.* **18** 401–24

[2] Jao J K 1994 A matched array beamforming technique for low-angle radar tracking in multi-path propagation model *IEEE Natl Radar Conf.* pp 171–6

[3] Gingras D F, Gerstoft P and Gerr N L 1997 Electromagnetic matched field processing: basic concepts and tropospheric simulations *IEEE Trans. Antenna Propag.* **45** 1357–545

[4] Papazoglou M and Krolik J 1999 Matched field estimation of aircraft altitude from multiple over-the-horizon radar revisits *IEEE Trans. Signal Process.* **47** 966–76

[5] Weaver J T 1967 The quasi-static field of an electric dipole embedded in a two-layer conducting half-space *Can. J. Phys.* **45** 1981–2002
[6] Holtham P, Richards T, Lucas C, le Grand M, Donati R and Bruxelle J Y 1999 Mesurements and propagation modeling in shallow water *Proc. Int. Conf. on Marine Electromagnetics MARELEC (Brest, France)*
[7] Gerstoft P 1994 Inversion of seismoacoustic data using genetic algorithms and *a posteriori* probability distributions *J. Acoust. Soc. Am.* **95** 770–82
[8] Gerstoft P and Mecklenbrauker C F 1998 Ocean acoustic inversion with estimation of *a posteriori* probability distributions *J. Acoust. Soc. Am.* **104** 808–19
[9] Dosso S E 2002 Quantifying uncertainty in geoacoustic inversion: I. A fast Gibbs sampler approach *J. Acoust. Soc. Am.* **111** 129–42
[10] Dosso S E and Nielsen P L 2002 Quantifying uncertainty in geoacoustic inversion: II. Application to broadband, shallow-water data *J. Acoust. Soc. Am.* **111** 143–59
[11] Dosso S E and Wilmut M J 2002 Quantifying data information content in geoacoustic inversion *IEEE J. Ocean. Eng.* **27** 296–304
[12] Mecklenbrauker C F and Gerstoft P 2000 Objective functions for ocean acoustic inversion derived by likelihood methods *J. Comput. Acoust.* **8** 259–70